

Green Synthesis of Nickel-rich $\text{Ni}_{0.89}\text{Co}_{0.08}\text{Al}_{0.03}\text{O}_2$ for Cathode material by Electrochemical Method

Adrian Nur^{1*}, Muthi'ah Syafa Gustian¹ and Novita Zita Primaresti¹

¹Chemical Engineering Department, Universitas Sebelas Maret, Jl Ir. Sutami 36 A Surakarta, Indonesia

Abstract. Nickel-rich layered oxides such as $\text{LiNi}_x\text{Co}_y\text{Al}_{1-x-y}\text{O}_2$ (NCA) are attractive cathode materials for lithium-ion batteries because they can deliver high energy density at reduced cobalt content. However, conventional co-precipitation routes typically require external acid/base dosing for pH control, which increases chemical consumption and generates salt-rich effluents. Here, we propose an electrochemical (acid-free) synthesis route using a bipolar-membrane electrolyzer to generate H^+ and OH^- in situ from water, thereby replacing reagent-based pH adjustment. A mixed Ni–Co–Al sulfate solution (Ni:Co:Al = 89:8:3) was processed at 60 °C and electrolyzed at 0.08 A cm^{-2} for 60 and 120 min. The resulting deposits were washed and dried, then lithiated with LiOH (Li:cathode precursor=1.05:1) and calcined (500 °C/6 h followed by 800 °C/20 h). SEM revealed hierarchical secondary aggregates with a flower-like morphology that became more consolidated at longer electrolysis time. EDS confirmed the presence of Ni, Co, and Al in the deposits. XRD showed reflections consistent with a layered NCA-type structure when compared with the reference card (JCPDS 87-1562), with the 120 min sample exhibiting sharper and better-resolved peaks; minor secondary phases were also detected, indicating incomplete phase purity under the present conditions. Overall, the bipolar membrane-assisted route demonstrates a feasible pathway to reduce external chemical inputs in Ni-rich cathode precursor synthesis, while highlighting the processing window required to strengthen phase formation toward layered NCA.

1 Introduction

Lithium-ion batteries (LIBs) are central to electric vehicles and grid-scale storage [1], intensifying the demand for cathode materials that deliver higher energy density while maintaining acceptable cost and safety. Ni-rich layered oxides, commonly expressed as $\text{LiNi}_x\text{Co}_y\text{Al}_{1-x-y}\text{O}_2$ (NCA), remain among the most promising candidates because increasing the Ni fraction raises practical capacity and reduces reliance on cobalt [2, 3]. However, achieving consistent performance from Ni-rich cathodes depends strongly on the precursor synthesis and the layered phase formation during lithiation and calcination.

Industrial NCA is typically produced via a two-step route: (i) synthesis of a transition-metal (TM) precursor (commonly hydroxide or carbonate) with controlled composition and secondary-particle morphology, followed by (ii) lithiation and high-temperature calcination to obtain the

*Corresponding author: adriannur@staff.uns.ac.id

layered oxide. Among available methods, co-precipitation is widely adopted because it can produce spherical secondary particles with a tunable size distribution. Nevertheless, conventional co-precipitation and hydrothermal routes [4-8] face several recurring challenges:

1. Reagent-intensive pH control and complexation. Precipitation is usually managed by repeated dosing with acids/bases (and often complexing agents such as ammonia) to regulate nucleation, growth, and homogeneity of composition. This increases chemical consumption and introduces variability when scale-up requires tight control of pH and supersaturation.
2. Salt-rich effluents and downstream burden. When sulfate or nitrate metal salts are used, external neutralization and pH adjustment generate large volumes of dissolved salts in the mother liquor (e.g., Na_2SO_4 or related by-products), which complicates washing, increases water demand, and raises wastewater-treatment load. Residual ions can also affect subsequent processing and impurity levels.
3. Reproducibility and composition drift. Differences in precipitation kinetics among Ni^{2+} , Co^{2+} , and Al^{3+} (including local pH microenvironments) can lead to compositional gradients or nonuniform distributions, which later influence calcination behavior, phase purity, and cation disorder.

These issues motivate alternative synthesis routes that reduce chemical dosing, lower waste generation, and still preserve control over composition and morphology.

From a sustainability and processing standpoint, acid usage (and more generally, reagent-based pH adjustment) can be problematic because it (i) increases the number of chemical inputs that must be handled and neutralized, (ii) produces additional ionic species that remain in the filtrate and require extensive washing, and (iii) can reduce the recyclability of process streams by increasing total dissolved solids and the complexity of the waste matrix. Consequently, claims of “green synthesis” for NCA precursors should be evaluated not only by the final product performance, but also by whether the route reduces external chemical consumption and minimizes salt-rich wastewater relative to conventional precipitation schemes.

Electrochemical processing provides a fundamentally different lever: ionic species can be generated in situ from water using electricity, enabling local pH control without direct addition of strong acids/bases. A bipolar membrane is particularly attractive because it can maintain separate acidic and alkaline environments by promoting water dissociation at the membrane interface, thereby creating H^+ and OH^- in different compartments. In principle, this allows precipitation and deposition phenomena to be driven by electrochemically controlled local chemistry, offering a pathway to (i) reduce reagent dosing, (ii) simplify downstream washing by lowering extraneous ions introduced from pH-control reagents, and (iii) enable coupling to renewable electricity.

In our previous work [9-10], we demonstrated electrochemical approaches for related materials processing and highlighted that electrochemical conditions strongly influence product characteristics. However, those studies did not critically address an acid-free bipolar membrane-enabled route specifically aimed at Ni-rich NCA-type precursor formation, nor did they systematically connect electrolysis time to deposit evolution, phase development after lithiation/calcination, and morphology relevant to NCA secondary-particle architecture. Therefore, a clear research gap remains: how bipolar membrane-driven in situ ionic generation can be used as a practical substitute for reagent-based pH control in Ni–Co–Al precursor synthesis, and how key electrochemical parameters govern the resulting precursor quality and the likelihood of forming the layered NCA phase.

This study aims to demonstrate an acid-free electrochemical synthesis route for Ni-rich NCA precursors using a bipolar-membrane electrolysis cell and to critically assess its potential sustainability advantage by comparing it with conventional reagent-driven precipitation in terms of chemical-input reduction and anticipated effluent complexity. Specifically, we evaluate the effect of electrolysis time on (i) the morphology and aggregation behavior of the formed deposits

(SEM), (ii) elemental incorporation (EDS as qualitative confirmation), and (iii) phase formation after lithiation and calcination (XRD), thereby strengthening the linkage between synthesis conditions, structure, and progression toward layered NCA.

2 Experimental

2.1 Materials

Aluminum sulfate hydrate ($\text{Al}_2(\text{SO}_4)_3 \cdot x\text{H}_2\text{O}$), cobalt(II) sulfate heptahydrate ($\text{CoSO}_4 \cdot 7\text{H}_2\text{O}$), nickel(II) sulfate heptahydrate ($\text{NiSO}_4 \cdot 7\text{H}_2\text{O}$), lithium hydroxide monohydrate ($\text{LiOH} \cdot \text{H}_2\text{O}$), and sodium hydroxide (NaOH) were purchased from Merck and used as received. Deionized water was used for all solution preparation and washing steps.

2.2 Bipolar-membrane electrolysis cell and operating conditions

Electrochemical synthesis was conducted in a two-compartment acrylic cell separated by a bipolar membrane (Fumasep FBM, FuMA-Tech). Two carbon electrodes were used as the anode and cathode. The effective membrane area exposed to the electrolyte was [$A_{\text{mem}} = 50 \text{ cm}^2$], and the electrode-to-membrane distance (or electrode spacing) was [$d = 3 \text{ cm}$] on each side. The cell was powered by a DC power supply operating under galvanostatic (constant current) control. To ensure mixing and minimize concentration gradients, the electrolysis cell was placed in an ultrasonic bath to provide continuous agitation during operation. No additional magnetic stirring was applied.

2.3 Electrochemical synthesis of Ni–Co–Al precursor (acid-free route)

A 1.0 M mixed sulfate solution (total volume 250 mL) containing Ni:Co:Al at a molar ratio of 89:8:3 was prepared and pre-heated to 60 °C under stirring for 30 min. Prior to electrolysis, the initial bulk pH was adjusted to 4.0 with 4.0 M NaOH.

Clarification of the “acid-free” concept: NaOH addition was used only to set a defined initial pH (pH 4) and to avoid uncontrolled bulk precipitation before electrolysis. No external mineral acid was added at any stage. The acidic/alkaline environments required for precipitation chemistry were generated in situ during bipolar-membrane operation via water dissociation and electrode reactions. In the anodic compartment, water oxidation produces protons (H^+), while in the cathodic compartment, water reduction generates hydroxide ions (OH^-). The resulting local pH gradients drive the formation of Ni–Co–Al hydroxide/oxyhydroxide deposits (precursor), replacing conventional reagent-based acid dosing. Electrolysis was performed at a current density of 0.08 A cm^{-2} for 60 and 120 min at 60 °C. After electrolysis, the solid deposits were collected, washed repeatedly with deionized water until the filtrate reached neutral pH, and dried in an oven at 120 °C. The dried powder is referred to as the Ni–Co–Al precursor (pre-lithiation).

2.4 Lithiation and calcination to form layered NCA

Lithium incorporation was performed after precursor formation. The dried Ni–Co–Al precursor was mixed thoroughly with $\text{LiOH} \cdot \text{H}_2\text{O}$ at a Li:cathode precursor molar ratio of 1.05:1 (i.e., 5% Li excess). The slight excess lithium was used to compensate for Li loss (e.g., volatilization and side reactions) during high-temperature treatment, a phenomenon commonly reported in layered Ni-rich cathode synthesis.

The powder mixture was first preheated at 500 °C for 6 h, followed by calcination at 800 °C for 20 h. The two-step heating protocol was selected because preheating to ~500 °C helps remove

residual water/hydroxyl species and promotes initial structural evolution before high-temperature crystallization, while the subsequent treatment near ~ 800 °C is widely used to develop the layered-type framework and improve the crystallinity of Ni-rich layered oxides. After calcination, the powder was cooled to room temperature naturally in the furnace and stored in a desiccator prior to characterization.

2.5 Lithiation and calcination to form layered NCA

X-ray diffraction (XRD) was used to identify crystalline phases on a Panalytical X'Pert Pro diffractometer with Cu $K\alpha$ radiation ($\lambda = 1.5406$ Å) operated at 30 kV. Scans were collected over $[2\theta \text{ range} = 15\text{--}70^\circ]$ with a step time of 0.7000 s.

Scanning electron microscopy with energy-dispersive X-ray spectroscopy (SEM/EDS) was used to examine morphology and qualitatively confirm elemental incorporation (Ni, Co, Al, O).

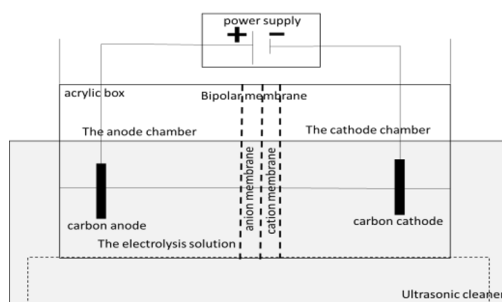


Fig. 1. The electrochemical NCA synthesis equipment

3 Result and Discussion

3.1 Precipitation of NCA

$\text{NiSO}_4 \cdot 7\text{H}_2\text{O}$, $\text{CoSO}_4 \cdot 7\text{H}_2\text{O}$, and $\text{Al}_2(\text{SO}_4)_3 \cdot x\text{H}_2\text{O}$ were used as metal-salt precursors to prepare the $\text{Ni}_{0.89}\text{Co}_{0.08}\text{Al}_{0.03}(\text{OH})_2$ cathode precursor by electrochemical method. The obtained transition-metal precursor was then mixed with LiOH and calcined to form the layered NCA cathode active material $\text{LiNi}_{0.89}\text{Co}_{0.08}\text{Al}_{0.03}\text{O}_2$. In this electrochemical method, researchers weigh Ni/Co/Al salts to a specific mole ratio to achieve a target transition-metal-layer composition of 0.89:0.08:0.03. However, precipitation can produce deviations (selective precipitation, complexation, Al loss, etc.), so the nominal composition must be verified. Cathode active material $\text{LiNi}_{0.89}\text{Co}_{0.08}\text{Al}_{0.03}\text{O}_2$ is hereinafter written simply as $\text{Ni}_{0.89}\text{Co}_{0.08}\text{Al}_{0.03}\text{O}_2$ in this paper.

NCA deposits form during electrolysis in the anode chamber. Oxidation of water at the anode, which releases H^+ ions, has successfully replaced the addition of acid in the NCA precipitation process, a method previously widely used. The remaining acid cannot be reused, making the process environmentally unfriendly. The role of chemical pH control is substituted by electrochemical generation of reactive species (H_2/H^+ and OH^-) from water, eliminating the need for external acid/base dosing. Conventional co-precipitation routes for NCA precursors typically rely on large amounts of external pH-adjusting chemicals (e.g., alkaline solutions and complexing agents) to drive and control hydroxide precipitation, which can generate salt-rich effluents and increase the chemical footprint. In this work, we replace reagent-based pH control with an electrochemically driven approach in which the precipitating base (OH^-) is produced in situ by cathodic water reduction ($2\text{H}_2\text{O} + 2\text{e}^- \rightarrow \text{H}_2 + 2\text{OH}^-$). The locally generated OH^- promotes the precipitation of Ni/Co/Al hydroxide species near the cathode without the need for equivalent

external base addition. As a result, the process can reduce the consumption of caustic/volatile reagents and may lower the ionic load of the mother liquor, potentially simplifying wastewater treatment. Moreover, because the driving force is electrical, the method can be coupled to renewable electricity, providing a pathway toward a more sustainable precursor synthesis. The process described in this paper uses the products of water oxidation to alter the acidic environment, thereby precipitating NCA. The remaining solution can still be used in the following process.

Figure 2 shows the morphology of NCA particles processed with a current density of 0.08 A/cm² for 60 and 120 minutes. Generally, both SEM images show the formation of micron-scale secondary aggregates with a flower-like (rosette-like) morphology, i.e., hierarchical particles composed of radially arranged plate-like subunits. Particles processed for 120 min appear larger and more agglomerated than those processed for 60 min. Longer electrolysis time provides more time for nano-sized primary particles (~10–100 nm) to nucleate and subsequently aggregate into micron-scale secondary particles (~1–5 μm), leading to larger observed aggregates.

The observed hierarchical aggregation is consistent with the general behavior of Ni-rich cathode precursors (e.g., NCA/NMC hydroxide or oxide-derived precursors), where nanoscale primary particles assemble into larger secondary particles. Such secondary-particle architectures are widely considered beneficial for electrode processing and performance because they can improve powder handling and tap density, enhance slurry rheology and coating uniformity, and reduce excessive surface area that may promote parasitic reactions. At the same time, the primary particle scale influences Li⁺ diffusion length and the degree of structural accommodation during cycling after lithiation/calcination. Therefore, controlling electrolysis time provides a practical handle to tune precursor aggregation, which may subsequently affect the microstructure of the lithiated/calcined layered NCA material and its electrochemical behavior.

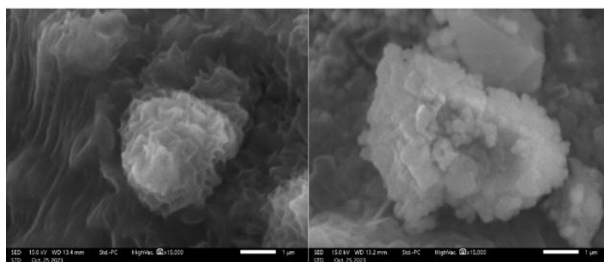


Fig. 2. The particle morphology of NCA

EDAX analysis of both deposits is shown in Table 1. The main NCA elements appear, namely Nickel, Cobalt, and Aluminum. SEM–EDAX (EDS) analysis (Table 1) confirms the presence of the main transition-metal elements associated with the NCA precursor, namely Ni, Co, and Al, together with O. Because EDAX is a local, semi-quantitative technique and the measured composition depends on the beam interaction location on heterogeneous deposits, the values in Table 1 should be interpreted as representative local compositions rather than strict bulk averages. Therefore, we use these results primarily to verify elemental incorporation and avoid quantitative comparison between the 60 min and 120 min samples based solely on point EDAX.

Table 1. The Elements in NCA particles

60 min time electrolysis		120 min time electrolysis	
element	mass (%)	element	mass (%)
O	61.21 ± 3.95	O	55.69 ± 0.90
Al	3.97 ± 0.96	Al	25.21 ± 0.56
Si	5.43 ± 1.08	Si	1.28 ± 0.14
S	5.51 ± 1.22	S	2.02 ± 0.16
Ni	20.77 ± 5.38	Ni	13.07 ± 1.03
Co	4.11 ± 0.89	Co	2.74 ± 0.37

It should be emphasized that SEM–EDX provides semi-quantitative, local elemental information, and the measured composition can vary significantly depending on the exact area where the electron beam interacts with a heterogeneous and porous deposit. Therefore, the EDX results in Table 1 are used primarily to confirm the presence of Ni, Co, and Al in the electrochemically formed deposits rather than to claim precise NCA stoichiometry or bulk composition. In particular, the apparent increase of Al from ~4 wt% (60 min) to ~25 wt% (120 min) is most reasonably attributed to spot-to-spot heterogeneity (e.g., the beam sampling Al-rich regions or Al-containing secondary domains) and matrix/topography effects that are well known in EDX analysis, rather than to a true uniform enrichment of Al throughout the sample. The detection of minor elements such as Si, S, and K suggests the presence of residual electrolyte/salt species, impurities from the precursor salts, or secondary phases (e.g., silicate-/sulfate-related species) that may remain after washing and can be locally concentrated in the deposit. Because EDX cannot quantify Li reliably and is not a robust method for validating the stoichiometry of Li-containing layered oxides, definitive compositional verification (including Li content and bulk Ni:Co:Al ratios) would require bulk analytical techniques such as ICP-OES/ICP-MS or XRF, which are recommended for future work.

3.2 Characterization of NCA

The X-ray diffraction pattern on NCA particles is shown in Figure 3. Figure 3 shows the XRD patterns of the deposits obtained at 60 and 120 min. Phase identification was performed by comparison with the standard reference card JCPDS 87-1562 for layered NCA. Both patterns exhibit the characteristic reflections of the NCA phase, with the 120 min sample showing more intense, better-resolved peaks. Minor additional reflections/peak shoulders suggest the presence of a small amount of secondary phases (impurities).

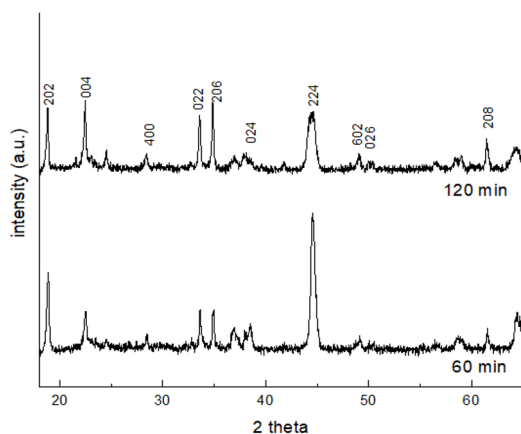


Fig. 3. XRD patterns of deposits obtained after 60 and 120 min. Peak positions and indices correspond to the layered NCA reference card (JCPDS 87-1562).

Phase identification in particles formed by the electrolysis process, with a current density of 0.08 A/cm² for 60 minutes, is shown in Figure 4. In contrast, Figure 5 shows phase identification in particles formed by the electrolysis process with a current density of 0.08 A/cm² for 120 minutes. The summary of phase identification results is shown in Table 2.

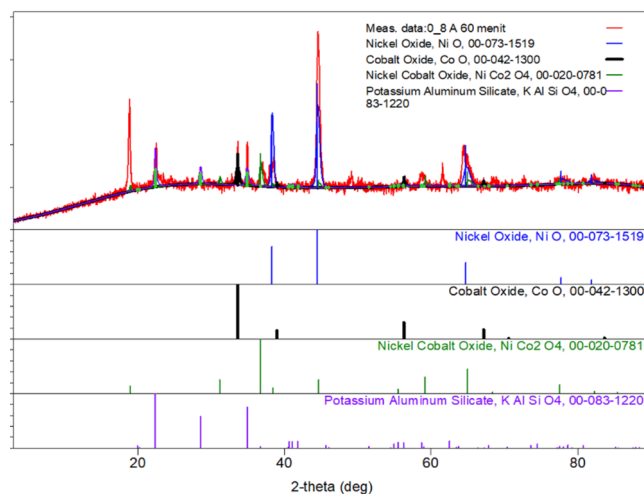


Fig. 4. Phase identification of synthesized NCA particles in 60 minutes

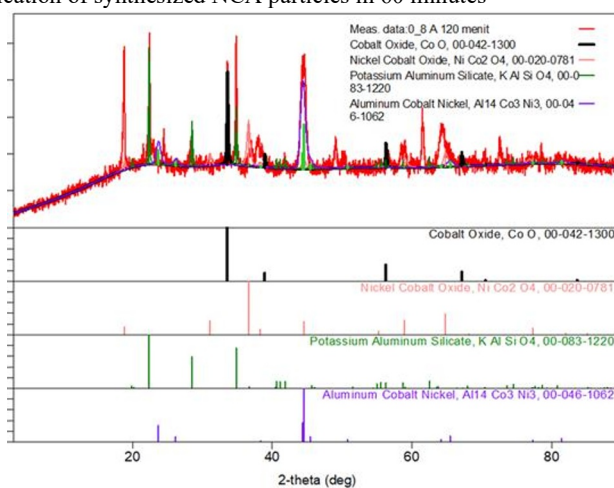


Fig. 5. Phase identification of synthesized NCA particles in 120 minutes

The electrolyzed particles for 60 minutes consisted of nickel oxide, cobalt oxide, nickel cobalt oxide, and potassium aluminum silicate. When the electrolysis time was increased to 120 minutes, nickel oxide was lost, and aluminum cobalt nickel appeared. Hence, the particles comprised cobalt oxide, nickel cobalt oxide, potassium aluminum silicate, and aluminum cobalt nickel. The percentage and size of crystallinity of each phase are shown in Table 2. It can be seen that crystallinity is generally still low, with crystal sizes of 4 - 150 Å. The electrochemical formation of NCA occurs in the anode chamber. The reaction in the anode chamber is an oxidation reaction. The longer the electrolysis time, the longer the oxidation time. This condition affects the particles formed. At an electrolysis time of 60 minutes, the particles formed were NiO. Increasing the electrolysis time to 120 minutes, NiO undergoes further oxidation and combines with Co to become NiCo₂O₄. The same thing happens to potassium and aluminum. After 60 minutes of electrolysis, only potassium aluminum silicate was formed. By increasing the electrolysis time to 120 minutes, potassium reacts with nickel and cobalt to form aluminum cobalt-nickel.

Table 2. Phase identification of electrochemically formed Ni–Co–Al deposits (pre-lithiation) at 60 and 120 min.

60 min time electrolysis			120 min time electrolysis		
Phase Identification	Crystallinity (%)	Crystallite Size (Å)	Phase Identification	Crystallinity (%)	Crystallite Size (Å)
Nickel Oxide, NiO	11.02	115	Cobalt Oxide, CoO	2.20	4.11
Cobalt Oxide, CoO	2.17	82.69	Nickel Cobalt Oxide, NiCo ₂ O ₄	12.2	142
Nickel Cobalt Oxide, NiCo ₂ O ₄	14.2	125	Potassium Aluminum Silicate, KAlSiO ₄	9.8	99
Potassium Aluminum Silicate, KAlSiO ₄	7.9	150	Aluminum Cobalt Nickel, Al ₁₄ Co ₃ Ni ₃	9.6	126

It is important to differentiate between the pre-lithiation electrochemically formed deposits and the final layered NCA cathode phase. In the pre-lithiation stage, the products can reasonably appear as a mixed oxide/oxyhydroxide system (e.g., NiO- and CoO-related phases and/or spinel-type Ni–Co oxides), because the electrochemical environment promotes local precipitation/deposition of transition-metal species without yet establishing the lithium-layered framework. The layered NCA structure (*R3m*) is expected to form only after lithiation and high-temperature calcination, during which Li incorporation and long-range cation ordering occur. Therefore, if the characteristic layered reflections are weak or not clearly resolved, this most likely indicates incomplete layered-phase development under the current processing conditions. Possible reasons include insufficient mixing or intimate contact between the precursor and LiOH, non-optimized calcination temperature/time and oxygen partial pressure, residual simple/spinel oxides that did not fully transform, and/or increased cation disorder (e.g., Ni/Li mixing) that can reduce the intensity and resolution of layered reflections. In this context, the XRD results are discussed as evidence of the phase evolution pathway and remaining secondary phases, highlighting that further optimization of lithiation and calcination parameters is required to strengthen the formation of phase-pure layered NCA.

4 Conclusion

The synthesis of NCA via electrolysis was successfully carried out. The water oxidation reaction, which produces hydrogen ions in the anode chamber, replaces the need to add acid to precipitate NCA particles. This process can avoid residual acid solution from the previous process. The composition of the resulting NCA particles demonstrates the suitability of the acid addition process for their formation.

References

1. Kotal, M., Jakhar, S., Roy, S., Sharma, H.K., *Journal of Energy Storage* **47**, 103534 (2022)
2. Jamil, S., Wang, G., Fasehullah, M., Xu, M., *Journal of Alloys and Compounds* **909**, 164727 (2022)
3. Zheng, X., Cai, Z., Sun, J., He, J., Rao, W., Wang, J., Zhang, Y., Gao, Q., Han, B., Xia, K., Xia, K., Sun, R., Zhou, C., *Journal of Energy Storage* **58**, 106405 (2023)
4. Entwistle, T., Sanchez-Perez, E., Murray, G.J., Anthonisamy, M., Cussen, S.A., *Energy Reports* **8**, 67–73 (2022)
5. Yudha, C.S., Hutama, A.P., Rahmawati, M., Arinawati, M., Aliwarga, H.K., Widiyandari, H., Purwanto, A., *Open Engineering* **12**, 501–510 (2022)

6. Wang, J., Zhou, G., Hou, S., Wei, S., Li, Y., Dong, S., Yan, X., Zhao, D., Hou, X., *Materials Letters* **335**, 133816 (2023)
7. Meghnani, D. and Singh, R.K., *Electrochimica Acta* **419**, 140403 (2022)
8. Wu, H., Pang, X., Bi, J., Wang, L., Li, Z., Guo, L., Liu, H., Meng, Q., Jiang, H., Liu, C., Wang, *Journal of Alloys and Compounds* **829**, 154571 (2020)
9. Nur, A., Budiman, A,W, Jumari, A., Nazriati, N., Fajaroh, F., *Chem. Chem. Technol.*, **15**, 3, 389–394 (2021)
10. Nur, A., Jumari, A., Dyartanti, E.R., Paramitha, T., Irianto, R.S., Ismarlian, H., Prahaspati, K., Kurniawan, L.A., *EVERGREEN*, **9**, 2, 421-426 (2022)